IEEE Access
Multidisciplinary | Rapid Review | Open Access Journal

Received March 16, 2020, accepted March 30, 2020, date of publication April 7, 2020, date of current version April 22, 2020.

Digital Object Identifier 10.1109/ACCESS.2020.2986309

The Power Simulation of Water-Cooled Central Air-Conditioning System Based on Demand Response

LIGAI KANG[1], **GANG WANG**[1], **YONGZHEN WANG**[2], **AND QINGSONG AN**[3]

[1]School of Civil Engineering, Hebei University of Science and Technology, Shijiazhuang 050018, China
[2]Department of Electrical Engineering, Institute of Energy Internet Innovation, Tsinghua University, Beijing 100084, China
[3]Key Laboratory of Efficient Utilization of Low and Medium Grade Energy, Tianjin University, Tianjin 300350, China

Corresponding author: Yongzhen Wang (wyz80hou@mail.tsinghua.edu.cn)

This work was supported in part by the Natural Science Foundation of Hebei Province under Grant E2019208191, in part by the Science and Technology Research and Development Plan of Shijiazhuang under Grant 205790085A and Grant 191060255, and in part by the Research fund for doctor supported by the Hebei University of Science and Technology under Grant 1181332.

ABSTRACT With rapid development of smart grid, terminal power load is paid more and more attention, especially that of air conditioning system, which constitute an integral part of summer peak electricity load. In this paper, through controlling indoor air temperature deduced by equivalent thermal parameters-model, daily energy consumption and energy consumption during peak hours can be adjusted and reduced to realize demand side management. To reduce peak load of grid and ensure stable and reliable operation of grid, four temperature control strategies, including constant setting temperature control strategy, pre-cooling control strategy, curtailment control strategy and improved curtailment control strategy were proposed. Meanwhile, three operation schemes of the chiller were also employed. Furthermore, considering the power consumption and curtailment, five indicators including hourly average load, hourly average load ratio, energy saving ratio, load-shedding ratio during peak hours and coefficient of performance (COP) have been proposed to evaluate the performance. Results showed that the operation scheme of operating numbers control obtained better effect. Energy saving ratio was highest of 32.5% with curtailment control strategy, while load-shedding ratio during peak hours was optimal with improved curtailment control strategy. However, COP was maximum at 3.66 when pre-cooling control strategy was employed. This study can guide the operation of water-cooled air conditioning system through energy saving ratio and COP, also it has more benefits on economy of power system by hourly average load and load-shedding ratio.

INDEX TERMS Load management, temperature control, power demand, operations research.

I. INTRODUCTION

With great development of economy and improvement of living standards, air conditioning system have been widely applied for meeting the demand of more comfortable living environment. Thus, it brings about a high proportion of power in terminal building's energy consumption. For public building in Guangzhou, air conditioning system accounts for a high percentage of electricity consumption, e.g., 43.2% for office building, 35.2% for shopping mall, 60.15% for hotel [1]. According to 2008 recommendation of Chinese People's Political Consultative Conference (CPPCC) in Guangzhou, the power consumed by air conditioning system accounts for 40% of total electricity usage in summer in Guangzhou.

Except for Northeast power grid and Northwest power grid, the peak load of other grids occurs at the period of high temperature in summer. Although more and more sustainable powered energy such as wind, solar, can be used [2], [3], with the increasing of air conditioning load, power grid load increases rapidly, which results in a larger gap between peak load and valley load. The rapid increasing of air conditioning load has been one of the main reasons on deterioration of grid load and power shortage. Therefore, it is very important to adjust air conditioning load within some extent. Liu *et al.* [4] put forwarded global energy intensity index firstly and then proposed the decomposition method which analyzes the influence of specific consumption and

The associate editor coordinating the review of this manuscript and approving it for publication was Cristina Rottondi.

delivered fluid ratios on global energy intensity. Siricharoenpanich *et al.* [5] studied the improvement performance of air conditioning system with cooling water loop for cooling refrigerant before entering the condenser unit. The obtained results showed that not only COP of air conditioning system were increased, but also the hot water storage was obtained. Zhou *et al.* [6] applied long short-term memory model to predict hourly energy consumption and daily energy consumption of air-conditioning systems in a library. Compared with the back propagation neural network prediction model and autoregressive integrated moving average model, results showed that the LSTM model acted more accurately.

To realize load-shedding and load-shifting in grid, Ai *et al.* [7] explored the load control management technology of central air conditioning system based on demand response. Zhang [8] studied the regulation measures and load analysis of air-conditioning based on power network in Shanghai. For purpose of a further substantive investigation on air conditioning load characteristics, and to explore effective measures of excessive increase of air conditioning load, we decide to carry out the research on load control technology of central air conditioning system based on demand response. Zhang *et al.* [9] has surveyed demand response research in deregulated electricity markets and Han *et al.* [10] has studied demand response based on information feedback. They both pointed out that lack of real time response of demand side would result in failure of California electricity market. Only if the demand side and supply side are equally treated, a stable electricity grid could be formed. Some studies [11]–[13] have pointed that the development of advanced metering infrastructure, modern control and optimization and wireless communication technologies lay a foundation for the demand response on the control of the demand side by supply side.

To realize the dynamic interaction of air conditioner and grid, Lu *et al.* [14]–[16] proposed a simplified equivalent thermal parameters model of a residential air conditioner to discuss the effect of a state queuing model, Schneider *et al.* [17] studied the impact of time-variant multi-state models on a single family residence and 8500-node test system using ZIP models and physical models, gave the simulation of indoor temperature and power consumed when the air conditioner was under different states (off, cooling, heating and auxiliary heating). Ji.Hoon Yoon *et al.* [18], [19] put forward the control strategy of changing the setting temperature by real time pricing. All above was often aiming at residential air conditioners, there was little study about controlling and scheduling of central air conditioning system and distributed energy system. Du [20] proposed the duty cycle control of central air conditioning system in lack-of-power situation during summer, analyzed the effect of duty cycle control to cooling load in summer in Nanjing in 2005. Xin and Wu [21] proposed an optimization model for remote duty cycle control of air conditioning system in business building by the advanced metering infrastructure.

To minimize energy consumption in a multi-chiller system, Coelho *et al.* [22], [23] proposed a new improved firefly algorithm based on Gaussian distribution function and differential cuckoo search algorithm to solve the optimal chiller loading design problem. Askarzadeh and Coelho [24] introduced the daily optimal chiller loading problem in which a 24-h cooling demand should be satisfied by a multi-chiller system (MCS) with the aim of minimizing total electrical power consumption of MCS. And then two particle swarm optimization (PSO) versions, namely, elitism-based PSO and multi-agent PSO were proposed to efficiently solve this problem. Lee *et al.* [25] employed differential evolution algorithm to solve the optimal chiller loading problem for reducing energy consumption. Powell *et al.* [26] presented a novel technique for solving a dynamic optimal chiller loading problem. The method reduced the complexity of the dynamic problem by considering all chillers to be a single, optimal chiller, which significantly reduced the number of decision variables. Tang *et al.* [27] developed an optimal control strategy which determined the number and schedule of operating chillers for precooling and particularly achieved an optimal cooling distribution among individual spaces. Yang *et al.* [28] presented a novel model predictive control developed for a dedicated outdoor air system-assisted separate sensible and latent cooling system. The model captured building thermodynamics, thermal comfort and air-conditioning and mechanical ventilation for building response prediction and energy use and thermal comfort optimization. Peng *et al.* [29] developed a novel remote-controlled system for use with air-conditioning units utilizing solid desiccant dehumidifiers which can be employed to create low carbon emission buildings. In the system, multiple information technologies such as sensor fusion, digital input/output communication and mobile technologies were employed to monitor and control the internal conditions of air-conditioned buildings and provide data collection, data processing, system control, and mobile access. Ai *et al.* [7] studied the load control technique of air conditioning system based on demand response, worked out a serie of load control strategies through the characteristics of cooling load, thus carried out some experimental research on load control strategy to explore its potential and prospect based on demand response. Considering matching the cooling, heating and electric output and the addition of new energy, Mancarella *et al.* [30] in 2013, put forward a black box model, including combined cooling, heating and power system, ground source heat pump system (GSHP) and boiler system. Under certain cooling heating and power demand, considering half hour pricing, different control strategies were employed whether GSHP or boiler were put into operation based on two kinds of gas price. Considering economic, environment and primary energy consumption, Kang *et al.* [13], [31], [32] proposed several control strategies to design the integrated energy system and also the optimal operation scheme was obtained by comparing the proposed control strategy with traditional control strategies, such as following electric load and following thermal load. As said in [21], the smart energy grid was constructed as well as the load control means of air conditioning system is explored.

As above, there are three kinds of remote load management: (1) interrupt control, i.e., the chiller will be shut-off remotely when system requires; (2) duty cycle control, which refers to the periodic on/off of the chiller; (3) temperature control i.e., users' thermostat is remotely controlled to achieve the control of cooling load. Among them, the latter two should be paid more attention and lead the future development direction for the advantages of its energy saving and friendly human thermal comfort requirement. In this paper the temperature control is adopted. And the main contribution of this paper is demand side management (DSM) based on equivalent thermal parameters-model, in which indoor air temperature is expressed by differential equations. Through controlling indoor air temperature, the daily energy consumption and energy consumption during peak hours can be adjusted and reduced to realize DSM.

The paper is organized as follows. The modeling of central air conditioning system is presented in section II, designed operation cases and evaluating indicators are introduced in section III. The modeling results are discussed in section IV. The conclusions are summarized in section V.

II. MODELING METHODOLOGIES

There are many types of central air conditioning system in China, such as air source heat pump system, water-cooled central air conditioning system, GSHP system, LiBr absorption refrigeration system. The conventional water-cooled central air conditioning system shown in Fig.1 is employed in this paper. The system includes three loops, which are refrigerant loop in cold water chiller, chilled water loop and cooling water loop.

The basic operating principle is as follows: in refrigerant loop, here are four main components: compressor, evaporator, condenser and throttle valve. Here, compressor is the most important component, it is the power source of heat conduction. Evaporator and condenser are the endothermic and exothermic transition components. Throttle valve is the control unit of the cold water chiller, which determines the evaporation pressure and condensing pressure. The refrigerant circulates between these components in a reverse Carnot cycle. In cooling mode, firstly, low-temperature and low-pressure liquid refrigerant in evaporator absorbs heat from chilled water at the other side of evaporator and evaporates into low-temperature and low-pressure superheated steam. Then, it is compressed into high-temperature and high-pressure gas through the compressor and afterwards it enters into condenser. In condenser, the gaseous refrigerant exchanges heat with cooling water in cooling water loop at the other side of condenser and releases heat to condense into a liquid of low temperature and high pressure. Finally, the liquid refrigerant passes through the throttle of expansion valve to reduce pressure, and turns into low-temperature and low-pressure liquid flowing into evaporator. Thus, a new cycle is starting.

In cooling water loop, it mainly consists of condenser, cooling water pump and cooling tower. Here, the cooling water is cooled by the fluid in the cooling tower and then

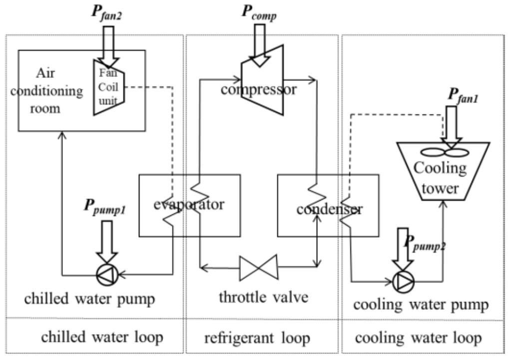

FIGURE 1. Schematic diagram of water cooled central air conditioning system.

sent to condenser of cold water chiller. In condenser, heat is exchanged with the high-temperature and high-pressure gaseous refrigerant to absorb heat, and the temperature raises. The cooling water is then sent to cooling tower by cooling water pump for cooling.

In chilled water loop, it is mainly composed of evaporator and chilled water pump. In evaporator, heat of chilled water from air conditioning room is exchanged with the liquid refrigerant of low temperature and low pressure, the temperature is lowered, and then flows back to the air conditioning room driven by chilled water pump.

In general, the power consumption of fan coil unit and cooling tower is much less than the chiller and water pump. So, these consumptions can be ignored. In addition, the temperature rising of water pump can also be ignored, there are three kinds of equipment to control, which are cold water chiller, chilled water pump, cooling water pump. Therefore, the load model of central air conditioning system can be illustrated by the model of cold water chiller and water pump. When indoor air temperature increase (or decrease), the load ratio of water chiller and water pump increase (or decrease) to response the changing temperature.

A. THE MODEL OF COLD WATER CHILLER

The chiller is the main energy consumption device in the central air conditioning system. Most of the year, it is operated under partial load. Therefore, it is very important to explore the energy saving potential of the air-conditioning system by studying the performance of the chiller under partial load and the matching relationship between the chiller under partial load and other parts of the air-conditioning system.

Fig.2 shows the influencing factors of the chiller's performance, that are cold water temperature and flow rate, cooling water temperature and flow rate, and cooling load. To establish the model of cold water chiller is to determine the influence of each parameter on the cooling capacity and power consumption of the chiller. As shown in Fig.2, the cooling load is influenced by two main factors: outdoor weather conditions such as outdoor air temperature, humidity and solar radiation, and indoor thermal disturbance, such as occupant

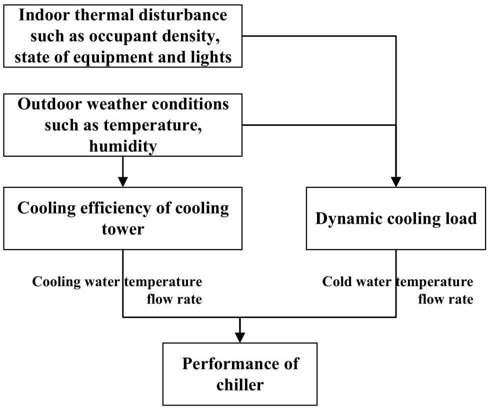

FIGURE 2. **Influencing factors of the chiller's performance.**

density, state of equipment and lights. Thus, cooling load is dynamic with the above change. In addition, the changing of outdoor weather conditions will result in cooling efficiency of the cooling tower. Corresponding to Fig.1, the cooling load is removed by the lowered cold water from the chiller and the heat is released to the air in the cooling tower by the cooling water from the chiller. Therefore, many other related influence factors are bringing out, such as chilled water temperature, cooling water temperature, cooling water flow rate, and chilled water flow rate, etc. In order to confirm the effect of each parameter to the cooling capacity and power consumption, the model of the cold water chiller is set up supplied by EnergyPlus using performance curves. And the performance curve are composed of three curves [33], [34], which are as follows:

1) COOLING CAPACITY CURVE

It is defined as the relation between the maximum cooling capacity and outlet temperature of the cooling water and chilled water, it is:

$$\begin{aligned} CAP_{AT} = a_1 + b_1 \times T_{ch,o} + c_1 \times T_{ch,o}^2 + d_1 \times T_{co,o} \\ + e_1 \times T_{co,o}^2 + f_1 \times T_{ch,o} \times T_{co,o} \end{aligned} \tag{1}$$

$T_{ch,o}$ the outlet temperature of chilled water (°C);

$T_{co,o}$ the outlet temperature of cooling water (°C);

$a_1, b_1, c_1, d_1, e_1, f_1$ coefficient (the same below).

So, the maximum cooling capacity running under the condition $T_{ch,o}$ and $T_{co,o}$ is:

$$Q_{\max} = Q_{eq} \times CAP_{FT} \tag{2}$$

$Q_{\max}$ the maximum cooling capacity (kW);

Q_{eq} the rated cooling capacity (kW).

2) THE RELATION CURVE OF COEFFICIENT OF PERFORMANCE (COP) AND RUNNING CONDITIONS

It is defined as the COP under maximum load changes with the outlet temperature of cooling water and chilled water, and it is:

$$COP_{FT} = 1 \Big/ \begin{pmatrix} a_2 + b_2 \times T_{ch,o} + c_2 \times T_{ch,o}^2 + d_2 \times T_{co,o} \\ + e_2 \times T_{co,o}^2 + f_2 \times T_{ch,o} \times T_{co,o} \end{pmatrix} \tag{3}$$

3) The relation curve of COP and part load ratio

It is defined as the COP changes with the part load ratio, and it is:

$$COP_{Fr} = 1 \Big/ \begin{pmatrix} a_3 + b_3 \times T_{co,o} + c_3 \times T_{co,o}^2 + d_3 \times r \\ + e_3 \times r^2 + f_3 \times T_{co,o} \times r + g_3 \times r^3 \end{pmatrix} \tag{4}$$

$$r = Q / Q_{\max} \tag{5}$$

r part load ratio;

Q real cooling capacity (kW).

Based on above three curves, the power consumption of the cold water chiller is:

$$P_{comp} = \frac{Q_{\max}}{COP_{eq}} \times \frac{1}{COP_{FT} \times COP_{Fr}} \tag{6}$$

P_{comp} the power consumption(kW);

COP_{eq} the rated coefficient of performance.

B. THE MODEL OF WATER PUMP

Under rated speed, the water pump performance curve is that the abscissa denotes the volume of water flow, and the ordinate can represent pressure head H, shaft power N, or efficiency of the pump.

When rotate speed changes, the performance parameters and performance curve will change, the change will follow the similarity law of water pump. Usually, some energy is consumed to overcome pressure difference, elevation difference and resistance while the fluid is flowing in the pipe. The fluid flow characteristics in the open pipeline system can be expressed as follows:

$$H = H_1 + SV^2 \tag{7}$$

H_1 basic head of opened system (m);

S pipe impedance (m/(kg/s)2);

V flow rate (kg/s).

In the closed piping system, such as cold water piping system $H_1 = 0$.

By the similarity law of water pump, the power can be calculated under different rotational speed and flow, thus the variable flow model describing the relation between P_{pump} and V can be obtained, which is as follows:

$$P_{pump} = a_4 + b_4 \times V + c_4 \times V^2 \tag{8}$$

C. THE MODEL OF COOLING TOWER AND FAN COIL UNIT

Here, power of cooling tower and fan coil unit in the system is assumed steady. And it is assumed to be 10% of power consumption of chiller and pump.

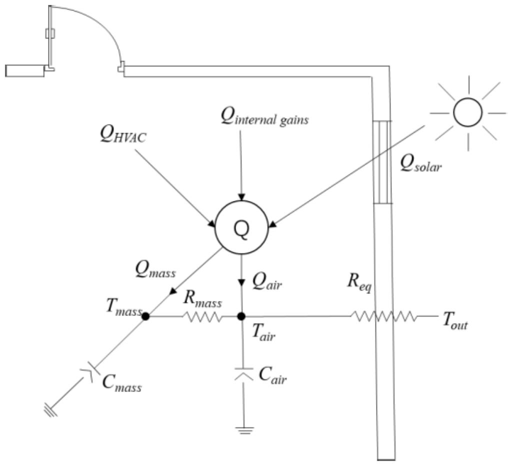

FIGURE 3. The heat flow in a typical room.

D. THE MODEL OF INDOOR AIR TEMPERATURE

Because the temperature control is employed in the following analysis of central air-conditioning control system, the calculation model of indoor air temperature is needed to set up. According to the first law of thermodynamics, this model can be constructed using an equivalent thermal parameter (ETP) model. Fig.3 shows the heat flow of a single room. As shown, it can be seen that the total heat Q is constituted by heat of three sources, including solar radiation through glasses Q_{solar}, internal gains from lights, equipment and bodies $Q_{internal\ gains}$, and supplied energy air conditioning system Q_{HVAC}. Then, the heat Q is divided by two parts: convective heat and radiant heat. Convective heat forms cooling load immediately, while radiant heat forms cooling load suffering from attenuation at a later time, that means this part of heat firstly transfers to interior surface, i.e., walls and furniture. When their temperature is higher than indoor air temperature, the heat transfers to the air. Therefore, heat Q is divided between the air Q_{air} and the mass such as walls and furniture in the room Q_{mass}. It is worth noting that indoor air temperature is thermally coupled to internal mass temperature, and then coupled to outdoor air temperature through envelope. Moreover, these heat transfers are unsteady and changing with outdoor air temperature, mode of lights and equipment and so on.

For the thermal circuit, if heat transfer properties are represented by equivalent electrical components with associated parameters, for indoor air temperature node and mass temperature node in Fig.3, the heat balance can be expressed as follows:

$$m\% \times Q - \frac{(T_{air} - T_{out})}{R_{eq}} - \frac{(T_{air} - T_{mass})}{R_{mass}} = C_{air} \times \frac{dT_{air}}{dt} \tag{9}$$

$$(1 - m\%) \times Q - \frac{(T_{mass} - T_{air})}{R_{mass}} = C_{mass} \times \frac{dT_{mass}}{dt} \tag{10}$$

C_{air} indoor air heat capacity (kJ/K);
C_{mass} mass heat capacity (kJ/K);
T_{out} outdoor air temperature (°C);
T_{air} indoor air temperature (°C);
T_{mass} mass temperature (°C);
R_{eq} the total thermal resistance of envelope (K/W);
R_{mass} the total thermal resistance of indoor material surface (K/W);
$m\%$ heat rate to air.

The detailed model is described in our previous work which were presented in international conference on applied energy in 2014 [35].

While the air conditioning system is on, the cooling capacity Q_{HVAC} is injected, otherwise, $Q_{HVAC} = 0$. Therefore, through the grid give some control signal at each time step to simulation model to control the air conditioning system on or off, it will make great effect on load shifting and stable operation of the grid.

TABLE 1. The operation scheme of the two chillers.

Operation scheme		Load ratio r >0.75	>0.625	>0.5	>0.25	>0.125	>0	=0
1	Chiller 1	1	0.75	0.75	0.5	0.25	0.25	0
	Chiller 2	1	0.75	0.75	0.5	0.25	0.25	0
2	Chiller 1	r	r	r	r	0.25	0.25	0
	Chiller 2	r	r	r	r	0.25	0.25	0
3	Chiller 1	1	1	1	2r	2r	0.25	0
	Chiller 2	2r-1	2r-1	0.25	0	0	0	0

III. CASE STUDY

A. THE DESIGNED OPERATION CASES

In actual use, cold water chiller is operated under partial load ratio for most of the time even in one day. The performance under partial load should be highly concerned. Therefore, two or more chillers are often employed to cool or heat simultaneously [36], the reasons are mainly as follows:

(1) Make the system operating more safely. When one chiller is in trouble, others can run continuously, thus the negative effect on system can be reduced.

(2) Make the system efficiency higher. When building load is lower, if only one chiller has been employed, the chiller must be running at lower load ratio; if more smaller chillers are employed, one of them can be turned off to make other units running at full capacity or high load ratio.

(3) Reduce the capacity of the standby chiller.

(4) Broaden the adjusting range of the load and prevent the surge phenomenon happening on centrifugal chiller.

Based above, two chillers "Carrier 23XL 724kW 6.04COP" used in a hotel in Guangzhou are selected in our work. Table 1 shows the three designed operation schemes of the two chillers. In each operation scheme, the load ratio of each chiller is set according to the building load ratio. Following the methods of ARI550 IPLV calculating, the chillers are assumed to work at load ratio of 100%, 75 %, 50%, 25% in operation scheme 1 or between the range of these load ratio in operation scheme 2 and operation scheme 3. It is worth

TABLE 2. **The four control strategies and their setting temperature.**

Control strategy	0-700 min	701-800 min	801-1000 min	1001-1440 min
1 constant setting temperature control strategy	26	26	26	26
2 pre-cooling control strategy	26	24	26	26
3 curtailment control strategy	26	26	28	26
4 improved curtailment control strategy	26	24	28	26

TABLE 3. **The designed twelve cases for modeling.**

Cases	Operation scheme	control strategy
Case 1	Operation scheme 1	control strategy 1
Case 2	Operation scheme 1	control strategy 2
Case 3	Operation scheme 1	control strategy 3
Case 4	Operation scheme 1	control strategy 4
Case 5	Operation scheme 2	control strategy 1
Case 6	Operation scheme 2	control strategy 2
Case 7	Operation scheme 2	control strategy 3
Case 8	Operation scheme 2	control strategy 4
Case 9	Operation scheme 3	control strategy 1
Case 10	Operation scheme 3	control strategy 2
Case 11	Operation scheme 3	control strategy 3
Case 12	Operation scheme 3	control strategy 4

noting that the minimum load ratio of chiller is set at 25% because of lower performance.

From table 1, it can be seen that for operation scheme 1 and operation scheme 2, the load ratio of each chiller changes simultaneously with the load ratio of building, the chillers are adjusted like a single chiller with larger capacity. Under this condition, the two chillers are both open. The difference of the two operation schemes is that the load ratio of chiller changes continuously under operation scheme 2, while under operation scheme 1, the load ratio of chiller is only allowed to operate at 100%, 75 %, 50%, 25%. For operation scheme 3, the number of operating chillers is firstly controlled, then, the load ratio of chiller is adjusted to adapt the variation of building load.

Table 2 shows the four control strategies designed with different set point of indoor air temperature. Under constant setting temperature control strategy, setting temperature is at 26 °C during all day. While setting temperature is at 24 °C within 700-800 min and 26 °C in other times under pre-cooling control strategy; under curtailment control strategy, setting temperature is at 28 °C within 800-1000 min and 26 °C in other times. Improved curtailment control strategy combines both above strategies, in which setting temperature is at 24 °C within 700-800 min, 28 °C within 800-1000 min and 26 °C in other times. Here, the fluctuation range of indoor air temperature are controlled under ±2° [37], [38]. Combining above three designed operation schemes and four control strategies, twelve cases shown in table 3 are proposed. In the following, the result of case 1 is selected as the benchmark to analyze the changing of power and other performances.

B. EVALUATING INDICATORS

In order to evaluate the effects of different control strategies, the following parameters are proposed.

1) HOURLY AVERAGE LOAD

It is used to evaluate the energy consumption of air conditioning system under different cases.

$$P_{ave} = \frac{\int_0^{1440} Pow_t dT}{24} \tag{11}$$

P_{ave} hourly average power (kW);

Pow_t the average power at t$^{\text{th}}$ min (kW).

2) HOURLY AVERAGE LOAD RATIO $\eta_{P_{ave}}$

It is used to evaluate the degree close to full load under different cases.

$$\eta_{P_{ave}} = \frac{P_{ave} \times 60}{\max\limits_{1 \le t \le 1440} Pow_t} \times 100\% \tag{12}$$

3) ENERGY SAVING RATIO η_{total}

$$\eta_{total} = \frac{\int_0^{1440} Pow_{ori,t} dt - \int_0^{1440} Pow_{lat,t} dt}{\int_0^{1440} Pow_{ori,t} dt} \times 100\% \tag{13}$$

$Pow_{lat,t}$ the power consumption when operating new case (case 2 to case 12) (kW);

$Pow_{ori,t}$ the power consumption when operating basic case (case 1) (kW);

4) LOAD-SHEDDING RATIO DURING PEAK HOURS

$$\eta_{Peak} = \frac{\int_{t_s}^{t_e} Pow_{ori,t} dt - \int_{t_s}^{t_e} Pow_{lat,t} dt}{\int_{t_s}^{t_e} Pow_{ori,t} dt} \times 100\% \tag{14}$$

η_{Peak} load-shedding ratio during peak hours

t_s the start time of the peak hours

t_e the end time of the peak hours.

5) COEFFICIENT OF PERFORMANCE (COP)

It is usually used to evaluate the performance of the chiller.

$$COP = \frac{\int_0^{1440} Cap_t dt}{\int_0^{1440} Pow_t dt} \times 100\% \tag{15}$$

Cap_t the average capacity at t$^{\text{th}}$ min(kW).

C. SIMULATION TESTS

The outdoor parameters of highest daily average temperature in typical year are selected as the basis of load calculating, outdoor dry and wet bulb temperature and solar radiation are shown in Fig.4. As seen, the solar radiation in 650-850 min is higher. Due to the hysteresis of radiation, the outdoor temperature in 800-1000 min has a higher value, the highest outdoor temperature is 36.6° at 900 min. So, at this time, natural indoor air temperature will be higher. When air conditioning system

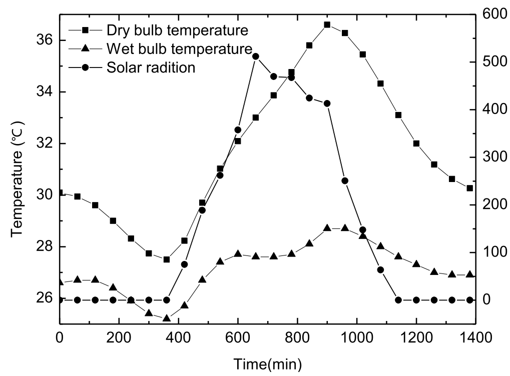

FIGURE 4. Outdoor weather conditions.

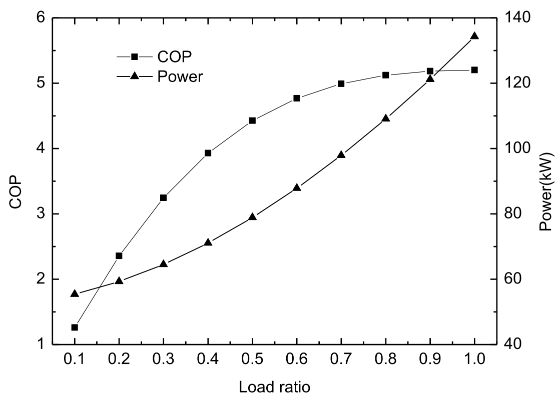

FIGURE 5. COP and power under part load ratio.

is used to cool indoor air at this time, power consumption may be very high. The research in the following is mainly discussing the power consumption in a day and during peak hours, which is in 800-1000 min.

Moreover, wet bulb temperature fluctuates between 25.2 °C and 28.7 °C within a day, volatility is far less than dry bulb temperature, and the values were also greater than that of design standard for energy efficiency of public building or ASHRAE standard using to calculate IPLV under 75% load. Thus, the effect of outdoor wet bulb temperature on cooling water is not considered. The designed outlet temperature of chilled water is set at 7 °C and cooling water temperature is set at 37 °C. Fig.5 shows the COP and power consumption changing with part load ratio.

IV. RESULTS AND DISCUSSION

A. INDOOR TEMPERATURE PROFILES AND POWER CONSUMPTION

According to the four control strategies, the changing of indoor air temperature is shown in Fig.6. And table 4 shows the running time and on-off number.

From Fig. 6, whatever control strategy is employed, it can be concluded that with the rising of outdoor air temperature or more absorbed solar radiation, indoor air temperature is rising until it reaches the upper controlled temperature. Here, compressor starts to work. Correspondingly, indoor air temperature is declining until it reaches the lower controlled temperature. Then compressor stops to work. Indoor air temperature is rising too, and so on. Such, indoor air temperature fluctuates between the upper controlled temperature and lower controlled temperature. Also, it can be seen that in the early morning, the outdoor temperature is low, the curve is relatively sparse, on-off frequency is also slow, even the chiller can stop for a longer time while indoor temperature can be still maintained at the required temperature. With the increase of outdoor temperature and solar radiation, curve is becoming denser, the on-off frequency also becomes quick.

TABLE 4. The running time and on-off number of compressor.

Control strategy	Running time		On-off number	
	Daily	801-1000 min	Daily	801-1000 min
Constant setting	622	112	21	5
Pre-cooling	559	101	21	4
Curtailment	567	80	21	4
Improved curtailment	545	69	20	3

Combined with table 4, it can be seen that compared with results of constant setting temperature control strategy, when pre-cooling control strategy is employed, some cooling is stored with 700-800 min ahead, running time during peak hours reduces from 112 min to 101 min, and the daily running time reduces from 622 min to 559 min. Meanwhile, on-off number also reduces by 1 time. The indoor air temperature is fluctuating between 22-26 °C within 700-800 min and 24-28 °C in other time of the day. While curtailment control strategy is used, indoor air temperature can maintain between 24-28 °C all day except for peak hours between at 26-30 °C. Compared with the results of constant setting temperature control strategy, the daily running time reduces by 55 min. Moreover, because the setting temperature is at 28 °C within 800-1000 min, higher than 26°C in constant setting temperature control strategy, running time during peak hours reduces by 32 min. If improved curtailment control strategy is employed, indoor air temperature is fluctuating between 24-28 °C all day except for peak hours between at 26-30 °C and 700-800 min before peak hours between at 22-26 °C. The daily running time and running time during peak hours decreases by 12.4% and 38.4%, respectively. Here, on-off number decreases to 3 times. So, to reduce the power consumption during peak hours, it is effective to improve the set point in this time or reduce the setting temperature to refrigerate ahead.

B. POWER CONSUMPTION OF DESIGNED CASES

Fig.7 shows the daily power consumption of twelve cases. From Fig.7, it can be seen that in case 2, because of the lower setting temperature 24 °C within 700-800 min, the curve is dense, and running time of high load ratio (higher than or equal to 75%) increases during this time. In addition, some cooling energy is stored ahead. When setting temperature is set back to original high temperature 26 °C, curve becomes sparse, the running time of high load ratio reduces to 42 min and power consumed is less than that in case 1.

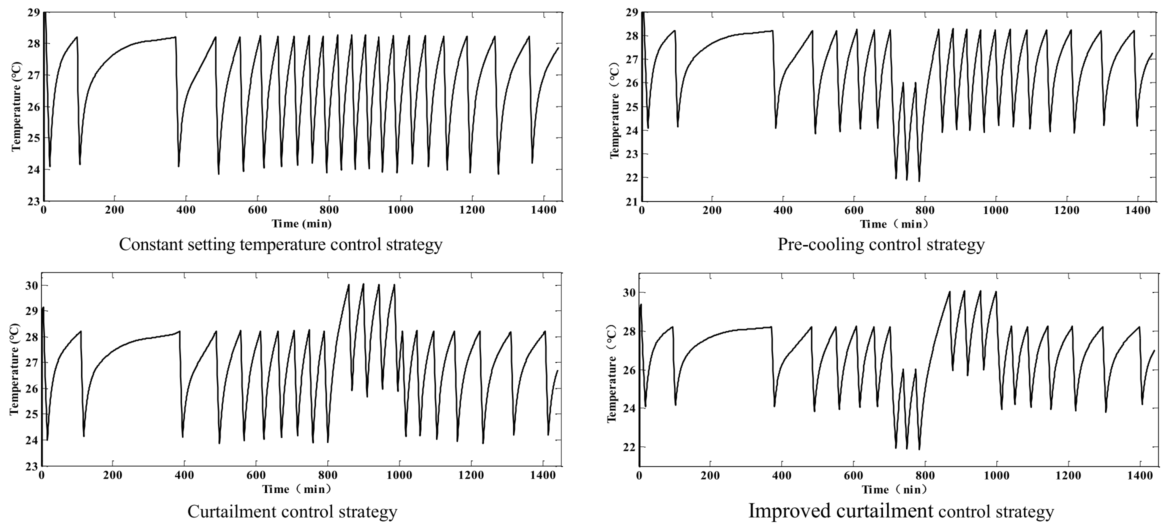

FIGURE 6. Indoor air temperature under different control strategies.

In case 3, because of the higher setting temperature within 800-1000 min, the curve is sparser during this time, the running time of high load ratio reduces from the original 50 min in case 1 to 37 min. When the setting temperature is set back to the original setting temperature, curve becomes dense and more power will be consumed to offset heat storage before.

In case 4, Because pre-cooling and curtailment control strategy are used simultaneously, the cooling capacity is stored firstly within 700-800 min, and then released. The running time of high load ratio dramatically reduce to 31 min during peak hours and consumed power is least. Similar changes are shown in case 5 to case 8 and case 9 to case 12.

From the perspective of different schemes, it can be seen that if the load ratio of building is below 0.25, the results of operation scheme 1 and operation scheme 2 are the same. Once building load ratio of is above 0.25, the power consumption changes continuously under operation scheme 2, while under operation scheme 1, the power consumption is a step function of load ratio. Therefore, the power consumption of operation scheme 2 will be lower than that of operation scheme 1. If operation scheme 3 is employed, power is consumed less than that of operation scheme 1 and operation scheme 2 at the same building load ratio. The reason is that one chiller can be closed at lower building load ratio and thus the other chiller can be operated at high load ratio. Even if the two chillers are both operated because of higher building load ratio, comprehensive performance may be better than that of operation scheme 1 and 2.

Table 5 gives the daily power consumption, power consumption during peak hours and COP. The detailed analysis will be proposed in the following section.

C. EVALUATING INDICATORS OF TWELVE CASES

Fig.8 - Fig.13 show the results of the proposed indicators.

Seen from Fig.8 to Fig.13, under different control strategies, the change law of each indicators is different.

TABLE 5. System power consumption of each case.

Cases	Daily power consumption (kW)	Power consumption in 800-1000 min (kW)	COP
Case 1	1971.5	421.4	3.308
Case 2	1865.3	376.4	3.135
Case 3	1852.7	306.6	3.579
Case 4	1816.9	285.4	3.409
Case 5	1797.1	361.1	3.275
Case 6	1757.7	361.4	3.655
Case 7	1679.4	265.2	3.388
Case 8	1705	270.3	3.211
Case 9	1385.8	316.6	3.601
Case 10	1402.1	299.2	3.391
Case 11	1331.6	232.1	3.263
Case 12	1351.7	223.2	3.664

From Fig.8 and table 5, it can be seen that hourly average load and daily power consumption of operation scheme 3 are lowest among that of the three operation schemes. If operation scheme 1 is employed, the hourly average load of constant setting temperature control strategy is highest, and the following is that of pre-cooling control strategy, curtailment control strategy and improved curtailment control strategy. While operation scheme 2 is employed, the hourly average load of four control strategies are 74.9 kW, 73.2 kW, 70.0 kW and 71.0 kW, respectively. And when operation scheme 3 is employed, the hourly average load of four control strategies are 57.7kW, 58.4 kW, 55.5 kW and 56.3 kW, respectively. The reason of this more or less consumption is that setting temperature of pre-cooling control strategy is 24 °C within 700-800 min, lower than that of constant setting temperature control strategy, the setting temperature of curtailment control strategy is 28 °C within 800-1000 min, higher than that of constant setting temperature control strategy, the setting temperature of improved curtailment control strategy is 28 °C within 800-1000 min, higher than that of curtailment control strategy. Higher setting temperature will result in less power

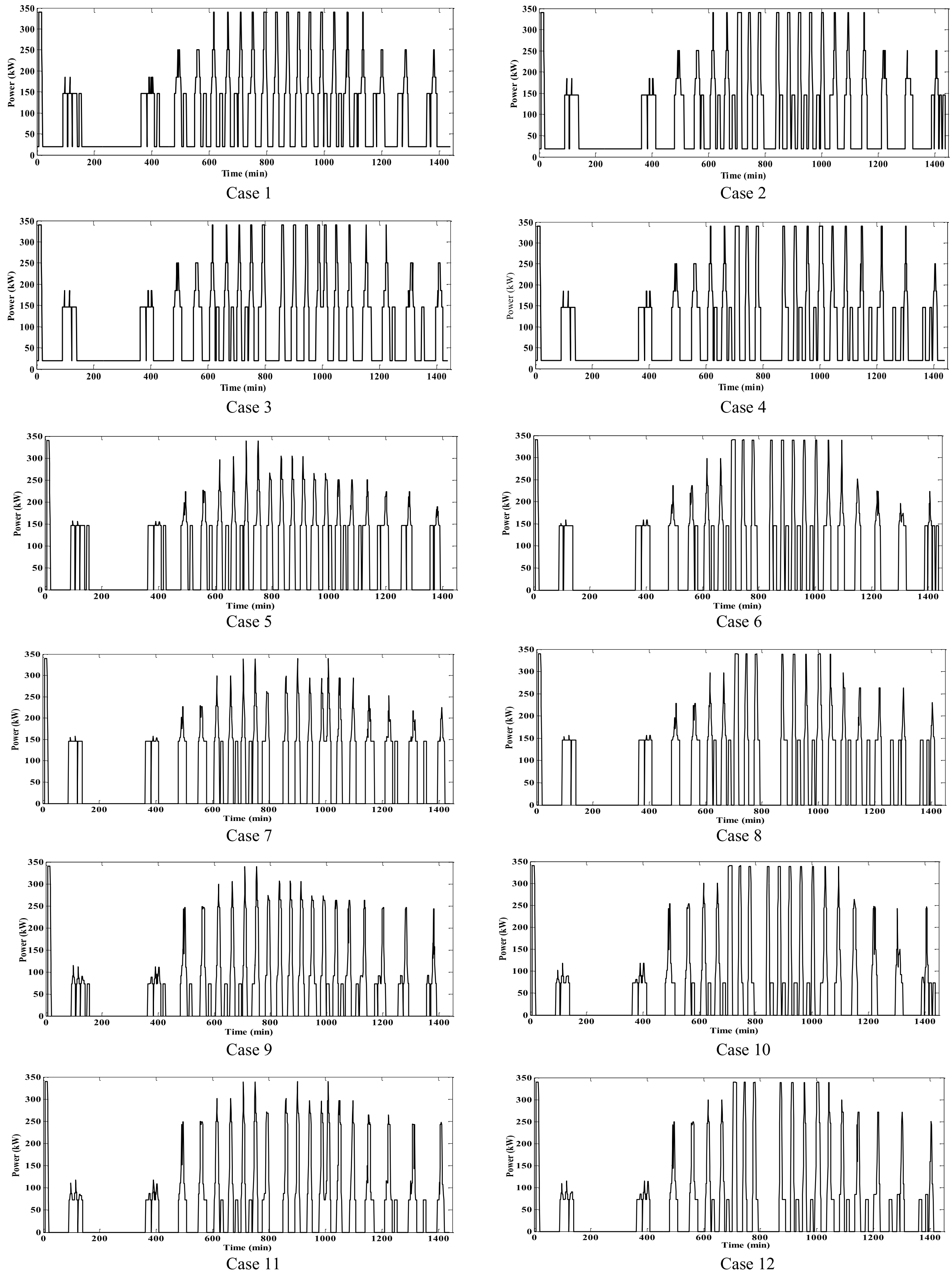

FIGURE 7. **Power consumption of twelve cases.**

consumption, and conversely lower setting temperature will result in more power consumption.

Fig.9 and Fig.10 show hourly average load ratio and energy saving ratio of each case. From Fig.9, it can be seen that

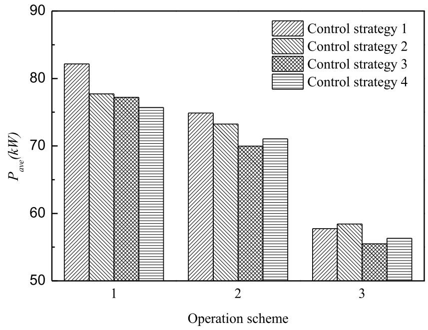

FIGURE 8. The hourly average load.

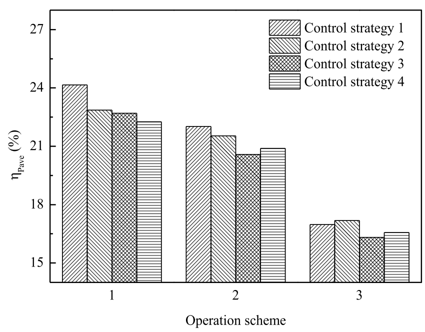

FIGURE 9. The hourly average load ratio.

the results of hourly average load ratio are similar with that of hourly average load. That is because in our simulation, whether which operation scheme or which control strategy is adopt, the maximum power is the power at full load ratio. If only a part of building load is met by the two chillers, the result may be different. In addition, one of the chiller or two chillers may be off at the lower building load ratio, hourly average load ratio is relatively low. And the highest value is 24.2% by case 1. When number control is adopted, hourly average load ratio is relative lower and the lowest result is 16.3% by case 11.

Unlike hourly average load ratio, the energy saving ratio of each case is just opposite of hourly average load ratio. When case 1 is as the benchmark, the highest energy saving ratio is obtained by case 11, which is 32.5%. And the following is 31.4% of case 12.

As shown in Fig.11 and Fig.12, the change rule of different control strategy is similar among proposed operation schemes. However, the power during peak hours is consumed less and load-shedding ratio is shifted more during peak hours under operation scheme 3 whether which control strategy is adopted. Compared with power consumption of operation scheme 1, for control strategy 1 to control strategy 4, they are reduced by 44.5 kW, 62.2kW, 33.1kW and 47.1 kW, respectively. The power consumption during peak hours at base case 1 is maximum at 421.4 kW, while at case 12, it is minimum at 223.2 kW and load-shedding ratio during peak hours is maximum at 47.0%. The reason is that the setting

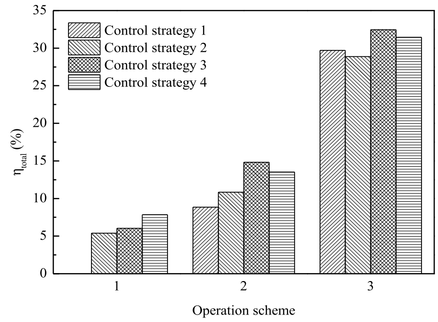

FIGURE 10. The energy saving ratio.

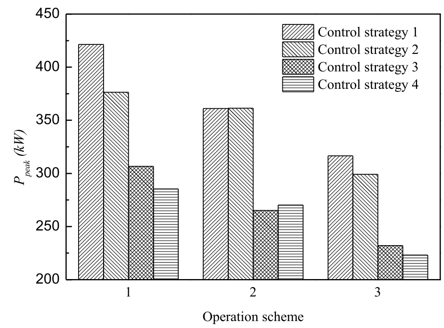

FIGURE 11. The power consumption during peak hours.

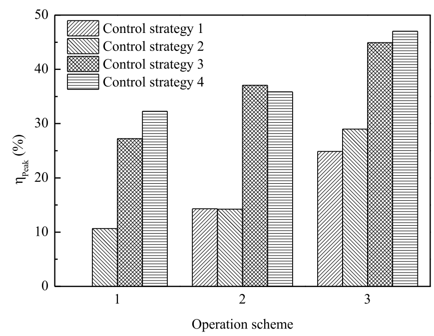

FIGURE 12. The load-shedding ratio.

temperature reduces to 24 °C ahead within 700-800 min, which can be storing a part of cooling; then the setting temperature increases to a new higher value 28 °C within 800-1000 min, the higher setting temperature will lead less power consumption.

Fig.13 gives COP of each case. It can be seen that COP of operation scheme 3 are highest among that of the three operation schemes. The following is that of operation scheme 1, operation scheme 2. That is because under operation scheme 3, when building load is lower, one chiller may be closed and the other chiller operates at high load ratio. While under operation scheme 1 and 2, both chillers are operated at lower ratio. Moreover, the chiller's load ratio of operation scheme 2 changes continuously, at the same building load ratio, the chiller may be operated at lower load ratio than that

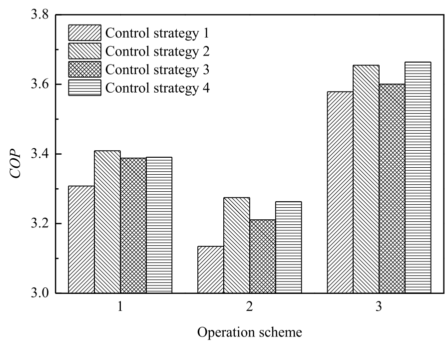

FIGURE 13. The coefficient of performance (COP).

of operation scheme 1. Thus, the performance of chiller may be worse and COP is lower.

Considering the control strategy, because COP is a ratio of cooling load to power consumption, the lower cooling load may result in lower power consumption, the difference of COP is not significant among each control strategies. the general order is COP of pre-cooling control strategy > COP of improved curtailment control strategy > COP of curtailment control strategy > COP of constant setting temperature control strategy. And the largest COP of each operation scheme are 3.41, 3.28, 3.66, respectively.

In conclusion, from results of above indicators, performances of operation scheme 3 are better than that of other two operation schemes. However, for each scheme, the results of every control strategy are different. They should be chosen according to the need, such as peak shedding effect or trying to make the system run at high load ratio, or maximum COP.

V. CONCLUSION

In view of large quantity of power load consumed by central air conditioning system, remote load control was adopted. In this paper, the power model of cold water chiller through performance curve and power - flow model of water pump were built, and then the effect of load ratio to the COP and power consumption was discussed under the designed twelve cases. Some results are obtained as follows:

(1) With different setting temperature of indoor air at different time, indoor air temperature can be controlled at required temperature. The fluctuation frequency is gradually reducing and running time of high load ratio reduces with the increase of the setting temperature.

(2) Performances of operation scheme 3 are better than that of other two operation scheme 1 with corresponding control strategy.

(3) Daily power consumption is lowest and energy saving ratio is highest under operation scheme 3 with curtailment control strategy, they are 1331.6 kW and 32.5%, respectively.

(4) About power consumption during peak hours and load-shedding ratio, the best performances are obtained by operation scheme 3 with improved curtailment control strategy. Compared with constant setting temperature control strategy under operation scheme 1, power consumption during peak hours reduced by 198.2 kW and load-shedding ratio is 47.0%.

(5) For each operation scheme, the largest COP is obtained by pre-cooling control strategy, they are 3.41, 3.28, 3.66, respectively.

REFERENCES

[1] Z. C. Liang, "Optimal design and economic analysis of CCHP based on public buildings in Guangdong," M.S. thesis, School Mater. Eng., Guangdong Univ. Tech., Guangzhou, China, 2013.

[2] X. Gao, B. Li, T. Wang, H. Sun, H. Yang, Y. Li, Y. Wang, and F. Zhao, "Investigation and validation of 3D wake model for horizontal-axis wind turbines based on filed measurements," *Appl. Energy*, vol. 260, Feb. 2020, Art. no. 114272.

[3] X. Gao, T. Wang, B. Li, H. Sun, H. Yang, Z. Han, Y. Wang, and F. Zhao, "Investigation of wind turbine performance coupling wake and topography effects based on LiDAR measurements and SCADA data," *Appl. Energy*, vol. 255, Dec. 2019, Art. no. 113816.

[4] L.-R. Liu, J.-J. Gu, and J. Liu, "Analysis of operational energy intensity for central air conditioning systems with water-cooled chiller by decomposition method," *Energy Buildings*, vol. 93, pp. 154–159, Apr. 2015.

[5] A. Sirichareonpanich, S. Wiriyasart, R. Prurapark, and P. Naphon, "Effect of cooling water loop on the thermal performance of air conditioning system," *Case Stud. Thermal Eng.*, vol. 15, Nov. 2019, Art. no. 100518.

[6] C. Zhou, Z. Fang, X. Xu, X. Zhang, Y. Ding, X. Jiang, and Y. Ji, "Using long short-term memory networks to predict energy consumption of air-conditioning systems," *Sustain. Cities Soc.*, vol. 55, Apr. 2020, Art. no. 102000.

[7] Z. Ai, Y. Q. Huang, and X. Yang, "Load control management technology of central air conditioning system based on demand response," *Pow. Commun. Manage. Smart Grid Commun. Tech. Proce.*, pp. 391–395, Apr. 2012.

[8] Z. Q. Zhang, "Regulation measures study and load analysis of air-conditioning base on power network in Shanghai," M.S. thesis, School Tech. Eco. Manage., North China Electric Power Univ., Beijing, China, 2007.

[9] Q. Zhang, X. F. Wang, and J. X. Wang, "Survey of demand response research in deregulated electricity markets," *Auto. Elec. Power Syst.*, vol. 3, no. 3, pp. 97–106, Mar. 2008.

[10] Y. J. Han, J. Q. Xin, and Y. L. Gao, "Demand responses based on information feedback," *Power Demand Side Manage.*, vol. 14, no. 5, pp. 9–14, May 2012.

[11] J. Y. Hu, E. Zhu, and X. G. Du, "Application status and development trend of power consumption information collection system," *Auto. Elec. Power Syst.*, vol. 38, no. 2, pp. 131–135, Feb. 2014.

[12] W. Sheng, C. Shi, J. Sun, B. Zhang, and T. J. Zhang, "Characteristics and research framework of automated demand response in smart utilization," *Autom. Electr. Power Syst.*, vol. 37, no. 23, pp. 1–7, Dec. 2013.

[13] X. Tian, S. Deng, L. Kang, J. Zhao, and Q. An, "Study on heat and power decoupling for CCHP system: Methodology and case study," *Appl. Thermal Eng.*, vol. 142, pp. 597–609, Sep. 2018.

[14] N. Lu, "An evaluation of the HVAC load potential for providing load balancing service," *IEEE Trans. Smart Grid*, vol. 3, no. 3, pp. 1263–1270, Sep. 2012.

[15] N. Lu and D. P. Chassin, "A state-queueing model of thermostatically controlled appliances," *IEEE Trans. Power Syst.*, vol. 19, no. 3, pp. 1666–1673, Aug. 2004.

[16] N. Lu, D. P. Chassin, and S. E. Widergren, "Modeling uncertainties in aggregated thermostatically controlled loads using a state queueing model," *IEEE Trans. Power Syst.*, vol. 20, no. 2, pp. 725–733, May 2005.

[17] K. P. Schneider and J. C. Fuller, "Detailed end use load modeling for distribution system analysis," in *Proc. IEEE PES Gen. Meeting*, Vancouver, BC, Canada, Jul. 2010, pp. 1–7.

[18] J. H. Yoon, R. Baldick, and A. Novoselac, "Dynamic demand response controller based on real-time retail price for residential buildings," *IEEE Trans. Smart Grid*, vol. 5, no. 1, pp. 121–129, Jan. 2014.

[19] J. H. Yoon, R. Bladick, and A. Novoselac, "Demand response for residential buildings based on dynamic price of electricity," *Energy Buildings*, vol. 80, pp. 531–541, Sep. 2014.

[20] X. J. Du, "Research of periodic stopping of central Air-conditioning technical in lack-of-power situation during summer," M.S. thesis, School Elect. Eng., Southeast Univ., Nanjing, China, 2006.

[21] J. Q. Xin and L. Wu, "Hierarchical strategies for duty cycling control of air conditioners in business buildings," *Auto. Elec. Power Syst.*, vol. 37, no. 5, pp. 49–54, May 2013.

[22] L. D. S. Coelho and V. C. Mariani, "Improved firefly algorithm approach applied to chiller loading for energy conservation," *Energy Buildings*, vol. 59, pp. 273–278, Apr. 2013.

[23] L. D. S. Coelho, C. E. Klein, S. L. Sabat, and V. C. Mariani, "Optimal chiller loading for energy conservation using a new differential cuckoo search approach," *Energy*, vol. 75, pp. 237–243, Oct. 2014.

[24] A. Askarzadeh and L. D. S. Coelho, "Using two improved particle swarm optimization variants for optimization of daily electrical power consumption in multi-chiller systems," *Appl. Thermal Eng.*, vol. 89, pp. 640–646, Oct. 2015.

[25] W.-S. Lee, Y.-T. Chen, and Y. Kao, "Optimal chiller loading by differential evolution algorithm for reducing energy consumption," *Energy Buildings*, vol. 43, nos. 2–3, pp. 599–604, Feb. 2011.

[26] K. M. Powell, W. J. Cole, U. F. Ekarika, and T. F. Edgar, "Optimal chiller loading in a district cooling system with thermal energy storage," *Energy*, vol. 50, pp. 445–453, Feb. 2013.

[27] R. Tang, S. Wang, K. Shan, and H. Cheung, "Optimal control strategy of central air-conditioning systems of buildings at morning start period for enhanced energy efficiency and peak demand limiting," *Energy*, vol. 151, pp. 771–781, May 2018.

[28] S. Yang, M. P. Wan, B. F. Ng, S. Dubey, G. P. Henze, W. Chen, and K. Baskaran, "Experimental study of model predictive control for an air-conditioning system with dedicated outdoor air system," *Appl. Energy*, vol. 257, Jan. 2020, Art. no. 113920.

[29] W. Peng, D. Su, and M. Higginson, "A novel remote control system for air conditioning in low carbon emission buildings using sensor fusion and mobile communication technologies," *Building Environ.*, vol. 148, pp. 701–713, Jan. 2019.

[30] P. Mancarella and G. Chicco, "Real-time demand response from energy shifting in distributed multi-generation," *IEEE Trans. Smart Grid*, vol. 4, no. 4, pp. 1928–1938, Dec. 2013.

[31] L. Kang, J. Yang, Q. An, S. Deng, J. Zhao, H. Wang, and Z. Li, "Effects of load following operational strategy on CCHP system with an auxiliary ground source heat pump considering carbon tax and electricity feed in tariff," *Appl. Energy*, vol. 194, pp. 454–466, May 2017.

[32] L. Kang, J. Yang, Q. An, S. Deng, J. Zhao, Z. Li, and Y. Wang, "Complementary configuration and performance comparison of CCHP-ORC system with a ground source heat pump under three energy management modes," *Energy Convers. Manage.*, vol. 135, pp. 244–255, Mar. 2017.

[33] W. P. Chen, "The optimization design and operation research of central air conditioning system," M.S. thesis, School Civil Eng., Hunan Univ., Changsha, China, 2008.

[34] ENERGY T U D O. (2007). *EnergyPlus V2.0 Manual*. [Online]. Available: https://simulationresearch.lbl.gov/modelica/releases/v2.1.0/help/Buildings_Fluid_Chillers_Data.html#Buildings.Fluid.Chillers.Data

[35] L. Kang, L. Liu, Q. An, J. Yang, J. Zhao, H. Jia, and D. Wang, "The equivalent thermal parameter model and simulation of air conditioner system in demand response programs," *Energy Procedia*, vol. 61, pp. 2004–2007, Jun. 2014.

[36] S. L. Liu and R. D. Chen, "New method of using IPLV to choose optimal refrigerating of dynamic load," *Fluid Machinery*, vol. 33, no. 8, pp. 63–66, Aug. 2005.

[37] *Design Code for Heating Ventilation and air Conditioning of Civil Buildings*, document GB 50736-2012, 2012.

[38] *Moderate Thermal Environments-Determination of the PMV and PPD Indices and Specification of the Condition for Thermal Comfort*, document GB/T 18049-2000, 2000.

LIGAI KANG was born in China, in 1983. She received the Ph.D. degree from the Key Laboratory of Efficient Utilization of Low and Medium Grade Energy, Tianjin University, Tianjin, China. She is currently with the School of Civil Engineering, Hebei University of Science and Technology. Her research interests include integrated energy systems, load forecasting, and demand side management.

GANG WANG was born in China, in 1978. He received the M.S. degree from the Qingdao University of Technology, Qingdao, Shandong, China. He is currently with the School of Civil Engineering, Hebei University of Science and Technology. His research interests include integrated energy systems, load forecasting, and demand side management.

YONGZHEN WANG was born in China, in 1987. He received the Ph.D. degree from the Key Laboratory of Efficient Utilization of Low and Medium Grade Energy, Tianjin University, Tianjin, China. He is currently with the Department of Electrical Engineering, Institute of Energy Internet Innovation, Tsinghua University, Beijing, China. His research interests include integrated energy systems, load forecasting, and demand side management.

QINGSONG AN was born in China, in 1979. He received the Ph.D. degree from Tianjin University, Tianjin, China. He is currently with the Key Laboratory of Efficient Utilization of Low and Medium Grade Energy, Tianjin University, Tianjin. His research interests include integrated energy systems, load forecasting, and demand side management.